Machine-Learning-Assisted Optimization of Type-II Superlattices for Enhanced Vertical Hole Mobility

1st John Glennon
Div. of Material Science and Engineering
Boston University
Boston, Massachusetts 02215, USA
ORCID: 0000-0001-8981-7786

2nd Enrico Bellotti
Dep. of Electrical and Computer Engineering
Div. of Material Science and Engineering
Boston University
Boston, Massachusetts 02215, USA
ORCID: 0000-0002-4747-8584

***Abstract*—Gaussian process regression is used to develop a model for predicting the superlattice (SL) structures grown on a 6.3 Å lattice. This model is used to search for optimized hole transport properties. Nonequilibrium Green's functions calculations are used to determine the vertical hole mobility of the structure which is compared with both the calculated and experimental results for an experimental SL grown on a GaSb substrate. Ultimately, a simple analytical model is used to approximate and compare the quantum efficiency of a photodiode containing each structure demonstrating an improvement in device performance using the optimized SL structure.**

***Index Terms*—quantum transport, carrier mobility, superlattices**

I. Introduction

Type-II Superlattices (T2SLs) are a promising material for use in infrared optoelectronics due to several potential advantages over bulk materials [1]. However, achieving high performance using these materials requires overcoming several fundamental disadvantages, such as poor vertical hole mobility [2] which can reduce photogenerated carrier collection in optoelectronic devices [1]. The parameter space of potential T2SL structures is massive when considering the layer thicknesses, alloy compositions, and substrate lattice constants. In this work, we search the parameter space of Ga-free T2SL structures for structures optimized for enhanced hole mobility and make predictions about the implications an optimized structure has on the performance of an IR photodiode (PD).

II. Methods

A. Band Structure Calculations

We use a four-band Hamiltonian that consists of the spin-up portion of the 8x8 $k \cdot p$ Hamiltonian within the axial approximation including the first conduction, heavy-hole, light-hole, and spin-orbit split-off bands. The Hamiltonian is expanded in first-order Lagrange polynomials via a finite-element procedure. The effect that strain induced in the material by lattice matching to a substrate has on the band structure is incorporated in the Hamiltonian as described in Ref. [3].

B. Quantum Transport

A problem-matched mode-space nonequillibrium Green's function formalism is utilized to calculate the transport properties of the SLs as detailed in Ref. [4]. Acoustic and polar-optical phonon scattering are included in the simulation via self-energies calculated according to the deformation potential and Fröhlich formalisms, respectively. Also, open boundary conditions are introduced via an additional self-energy term. The Green's functions are calculated by solving the Dyson and Keldysh equations self-consistently. Then, the mobility is extracted using resistance scaling analysis as outlined in Ref. [5].

III. Results and Discussion

We probe the parameter space of ideal Ga-free SLs lattice-matched to a substrate with a lattice constant of 6.3 Å calculating the band gap and the conductivity effective mass, as described in Ref. [6], for approximately 1,000 different SL structures. Then, we use Gaussian processes (GP) to perform nonparameteric regression on the data set selecting 100 structures that exhibit a cutoff wavelength of approximately $12.5\,\mu m$ and exhibit low conductivity hole effective mass. The band structure is calculated for these optimized SLs to confirm the cutoff wavelength. From this set of structures we select a 5/3 ML $InAs_{0.41}Sb_{0.59}$/$InAs_{0.03}Sb_{0.97}$ SL structure which exhibits the lowest hole effective mass for the desired cutoff wavelength. The calculated band structure of this optimized SL is compared with that of a 34/6 ML $InAs_{0.97}Sb_{0.03}$ /$InAs_{0.52}Sb_{0.48}$ SL structure on a GaSb substrate in Figs. 1b and 1a, respectively. This other SL is inspired by an experimentally realized structure with a $12.5\,\mu m$ cutoff presented in Ref. [7]. The band structures suggest that the optimized SL structure will exhibit a wide hole miniband which is advantageous for carrier transport.

Next, we run several NEGF simulations for both structures. Band diagrams of an example of the NEGF simulations used for each SL structure are presented in Fig. 2. It is clear that the hole barriers in the 5/3 ML $InAs_{0.41}Sb_{0.59}$/$InAs_{0.03}Sb_{0.97}$ SL structure are far thinner than those in the 34/6 ML $InAs_{0.97}Sb_{0.03}$ /$InAs_{0.52}Sb_{0.48}$ SL structure which also suggests superior hole transport properties assuming all other factors are equal. The vertical hole mobility is extracted and is plotted as a function of temperature in Fig. 3. The experimental vertical hole mobility from Ref. [7] is also included. The optimized structure exhibits calculated mobility values that are approximately three orders of magnitude higher than those

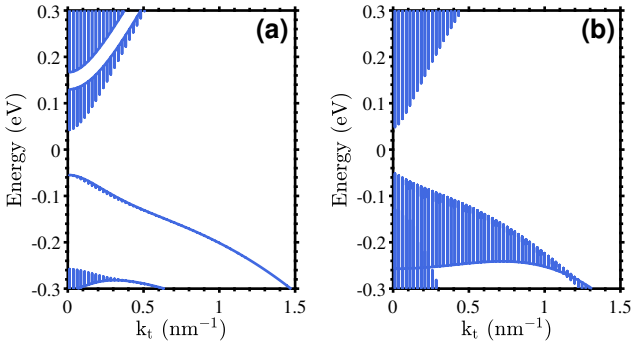

Fig. 1. The band structure calculated for the 34/6 ML $InAs_{0.97}Sb_{0.03}$ /$InAs_{0.52}Sb_{0.48}$ structure on a GaSb lattice (a) and the 5/3 ML $InAs_{0.41}Sb_{0.59}$/$InAs_{0.03}Sb_{0.97}$ structure on a 6.3 Å lattice (b). The vertical lines represent the dispersion with respect to the vertical wave vector.

of the experimental structure. The calculated mobility for the experimental structure is lower than the experimental results which is likely due to the greater confinement of holes in an ideal SL compared with a real SL.

Finally, we calculate an approximation for the internal QE for a simple PD based on the vertical hole mobility data presented in Fig. 3. Eq. (33) on page 676 from Ref. [8] was used assuming a minority carrier lifetime τ of 100 ns, an absorption coefficient α of 500 cm^{-1}, and an absorption layer thickness W_A of 2 μm with no reflection for both SLs. The results are plotted along with the mobility in Fig. 3. The PD based on the optimized SL exhibits far higher QE.

IV. Conclusion

To summarize, we used Gaussian process regression to predict optimized Ga-free SL structures for hole transport grown on a substrate with a 6.3 Å lattice constant. NEGF was use to calculate the vertical hole mobility for this structure as well as one that was inspired by an experimental structure. The optimized SL structure exhibits greatly enhanced hole mobility when compared with both the calculated and experimental results of the other SL structure, resulting in the prediction of enhanced internal QE of a simple PD using the optimized SL structure.

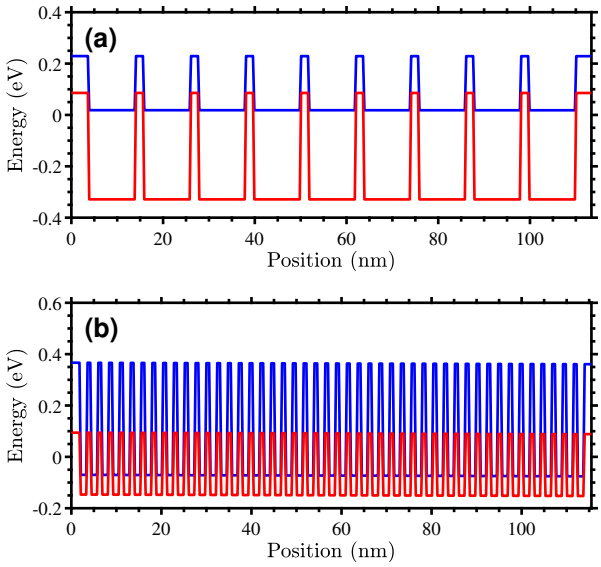

Fig. 2. The conduction (blue line) and valence (red line) bands for the 34/6 ML $InAs_{0.97}Sb_{0.03}$ /$InAs_{0.52}Sb_{0.48}$ structure on a GaSb lattice (a) and the 5/3 ML $InAs_{0.41}Sb_{0.59}$/$InAs_{0.03}Sb_{0.97}$ structure on a 6.3 Å lattice (b).

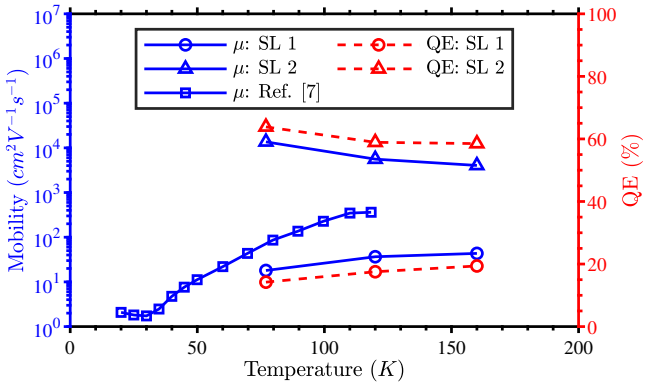

Fig. 3. The vertical hole mobility (blue lines) and internal QE (dashed red lines) calculated as a function of temperature for the 34/6 ML $InAs_{0.97}Sb_{0.03}$ /$InAs_{0.52}Sb_{0.48}$ structure on a GaSb lattice ("SL 1") and the 5/3 ML $InAs_{0.41}Sb_{0.59}$/$InAs_{0.03}Sb_{0.97}$ structure on a 6.3 Å lattice ("SL 2"). The experimental vertical hole mobility from Ref. [7] is also included.

References

[1] A. Rogalski, P. Martyniuk, and M. Kopytko, "Type-ii superlattice photodetectors versus hgcdte photodiodes," *Progress Quantum Electron.*, vol. 68, p. 100228, 2019.

[2] E. Bellotti, F. Bertazzi, A. Tibaldi, J. Schuster, J. Bajaj, and M. Reed, "Disorder-induced degradation of vertical carrier transport in strain-balanced antimony-based superlattices," *Phys. Rev. Appl.*, vol. 16, p. 054028, Nov 2021.

[3] P. Enders, A. Bärwolff, M. Woerner, and D. Suisky, "k·p theory of energy bands, wave functions, and optical selection rules in strained tetrahedral semiconductors," *Phys. Rev. B*, vol. 51, pp. 16695–16704, Jun 1995.

[4] F. Bertazzi, A. Tibaldi, M. Goano, J. A. G. Montoya, and E. Bellotti, "Nonequilibrium green's function modeling of type-ii superlattice detectors and its connection to semiclassical approaches," *Phys. Rev. Appl.*, vol. 14, p. 014083, Jul 2020.

[5] J. Glennon, F. Bertazzi, A. Tibaldi, and E. Bellotti, "Extraction of mobility from quantum transport calculations of type-ii superlattices," *Phys. Rev. Appl.*, vol. 19, p. 044045, Apr 2023.

[6] D. Z. Ting, A. Soibel, and S. D. Gunapala, "Hole effective masses and subband splitting in type-ii superlattice infrared detectors," *Appl. Phys. Lett.*, vol. 108, no. 18, p. 183504, 2016.

[7] B. V. Olson, J. F. Klem, E. A. Kadlec, J. K. Kim, M. D. Goldflam, S. D. Hawkins, A. Tauke-Pedretti, W. T. Coon, T. R. Fortune, E. A. Shaner, and M. E. Flatté, "Vertical hole transport and carrier localization in $\mathrm{InAs/inas}_{1-x}\mathrm{sb}_x$ type-ii superlattice heterojunction bipolar transistors," *Phys. Rev. Appl.*, vol. 7, p. 024016, Feb 2017.

[8] S. M. Sze, *Physics of Semiconductor Devices*. Hoboken, NJ: Wiley-Interscience, 3rd ed.. ed., 2007.